Kinetic performance of reversed-phase C18 high-performance liquid chromatography columns compared by means of the Kinetic Plot Method in pharmaceutically relevant applications

A. Fanigliulo [a], D. Cabooter [b,*], G. Bellazzi [a], B. Allieri [a], A. Rottigni [a], G. Desmet [b]

[a] GlaxoSmithKline R&D, Pharmaceutical Development, Via Fleming 4, 37135 Verona, Italy
[b] Vrije Universiteit Brussel, Department of Chemical Engineering, Pleinlaan 2, 1050 Brussels, Belgium

ARTICLE INFO

ABSTRACT

Four fully porous C18 columns (Hypersil Gold, ACE3, Xbridge and Gemini NX), widely employed in the pharmaceutical industry, were compared in terms of efficiency and analysis speed with the Kinetic Plot Method. Weakly basic, medium-sized, N-containing pharmaceutical compounds from GlaxoSmithKline Research and Development were used as test molecules. Isocratic elution was carried out at pH 4.5 and pH 8.0 with acetonitrile as organic modifier. The columns under evaluation included highly pure silica supports (Hypersil Gold, ACE3) and hybrid polymer-silica supports (XBridge, Gemini NX). Both types of columns claim for nearly absent secondary interactions with ionized silanol groups and are therefore applicable in a wide pH range. This is an important feature for method development purposes in pharmaceutical industries. The Kinetic Plot Method was used to compare the support characteristics and assess the kinetic performance of the columns in different experimental conditions. Although the evaluated columns have roughly identical particle diameters (from 3.0 to 3.5 μm) according to their manufacturers, large differences in kinetic performance were observed at pH 4.5 that can be accounted for by different flow resistances, porosities and average particle diameters, experimentally determined from scanning electron microscopy and laser light scattering experiments on loose stationary phase material. The ACE3 column was the best performing support among the evaluated columns, due to its excellent efficiency and average flow resistance. The better performance of the ACE3 column was due to its better packing quality, as could be derived from its impedance plot. Kinetic plots of resolution of a critical pair *versus* analysis time and column length were established at pH 8.0. These plots can be used as a method development tool to tailor the separation conditions to the required resolution of a given critical pair, combining efficiency and selectivity features of the column.

© 2010 Elsevier B.V. All rights reserved.

1. Introduction

Silica modified with chemically bonded alkyl chains is still by far the most widely employed stationary phase for HPLC reversed-phase (RP) columns. Alternative chromatographic supports, such as zirconia oxide [1,2] or fully polymeric materials [3] have in fact resulted in poorer efficiency, retentivity and mechanical resistance.

One of the main issues when producing RP silica columns is the control and limitation of unreacted or unshielded silanol groups that survive the end-capping procedure and can compete with purely hydrophobic interactions between analytes and the alkyl chains of the stationary phase through additional polar, adsorptive, ionic – especially at high pH, where they are deprotonated – or even repulsive interactions. These secondary interactions are usually detrimental to selectivity and separation efficiency, often leading to band broadening and peak shape distortion [4,5]. This phenomenon has a considerable impact particularly on the chromatography of nitrogen-containing ionisable compounds that currently represent the great majority of molecules of pharmaceutical and biochemical interest [6]. Mainly two processes are in place today in the development of chromatographic materials to reduce residual exposed silanol groups: the use of "Type B" deactivated ultra-pure silica, and the use of hybrid polymer-silica materials.

In this paper, the kinetic performance of two ultra-pure silica (Hypersil Gold from Thermofisher Scientific and ACE3 from Advanced Chromatography Technologies) and two polymeric silica (Gemini NX from Phenomenex and XBridge from Waters) supports of C18 HPLC analytical columns was evaluated and compared by using three research compounds from GlaxoSmithKline Research and Development as test molecules and the Kinetic Plot Method (KPM) as a tool for comparison and assessment of performance.

* Corresponding author. Tel.: +32 2 629 33 30; fax: +32 2 629 32 48.
E-mail address: dcaboote@vub.ac.be (D. Cabooter).

3352

A. Fanigliulo et al. / J. Chromatogr. A 1218 (2011) 3351–3359

The Hypersil Gold column is based on a proprietary derivatization and end-capping procedure of highly pure silica that claims to give reduced peak tailing, improved efficiency and pH stability. In particular, the manufacturer claims for high robustness at very low pH. Hypersil Gold stationary phases are widely used in the separation of pharmaceutical compounds [7] and metabolites [8], often in LC–MS applications [9].

ACE3, in spite of the less popular brand, is gaining appraisal in the pharmaceutical industry [10,11] for evidence of batch-to-batch reproducibility, extended column lifetime and high temperature and pH stability.

The XBridge phase, based on Bridged Ethyl Hybrid (BEH) technology, was the first hybrid silica column entering the market. It is prepared from two highly pure monomers (tetraethoxysilane and bis(triethoxysilyl)ethane) that lead to the formation of ethane bridges between Si atoms. It has attracted analysts' interest from its debut and it is now largely used in pharmaceutical companies [12].

Gemini NX is developed by a proprietary process that incorporates polymeric silica onto a pure silica substrate nucleus. Ethane ligands are embedded in the polymeric silica bridging the Si atoms. This structure is claimed to give highly extended pH stability and mechanical resistance at the same time [13].

All the tested columns are suitable for applications in a wide pH range, namely from pH 2.0 up to pH 11.0 (ACE3) or 12.0 (Hypersil Gold, XBridge, Gemini NX), which is a very frequently required characteristic in the pharmaceutical analysis field, allowing to scout a large spectrum of pH selectivities when developing new chromatographic methods. For this reason, the evaluation of the kinetic performance of the above columns was carried out both at slightly acidic (4.5) and basic (8.0) pH in order to highlight possible differences due to different support materials.

The molecules chosen as probes for the experiments carried out in this work are nitrogen-containing weak bases that are ionized at different pH values. They will be referred to as G1, G2 and G3 within the following text. Care was taken to evaluate the test molecules at a mobile phase pH that grants neutrality of the relevant molecule, in order to assess column efficiency in the absence of possible secondary non-hydrophobic interactions.

Due to their very similar structure, G2 and G3 form a potential critical pair in chromatographic methods for the detection and quantification of impurities of an active pharmaceutical compound. Therefore, the resolution between G2 and G3 was evaluated at pH 8.0 on the different columns under isocratic conditions, keeping the retention factor of the last eluting peak constant and evaluating differences in efficiency and intrinsic column selectivity at this pH.

The KPM was used to perform the column performance comparison described above [14–17]. Briefly, the KPM allows to transform any experimentally obtained (u_0, H)-couple, obtained in a column with permeability K_{v0}, into a (N, t_0)-couple for a certain value of pressure (ΔP) using the following equations:

$$N = \frac{\Delta P_{max} K_{v0}}{\eta u_0 H} \tag{1}$$

$$t_0 = \frac{NH}{u_0} = \frac{\Delta P_{max} K_{v0}}{\eta u_0{}^2} \tag{2}$$

with H the column plate height (μm) and K_{v0} the bed permeability (m²), defined as:

$$K_{v0} = \frac{u_0 \eta L}{\Delta P}, \tag{3}$$

u_0, the linear velocity of an unretained molecule (m/s); η, the viscosity of the mobile phase (Pa s) and L, the column length (m).

This (N, t_0)-couple represents the efficiency N that can be obtained in a certain time t_0 would the same support be used in

a column that is exactly long enough to generate the pressure ΔP at the given velocity u_0. Performing this data transformation for an entire set of van Deemter data, experimentally obtained on a column of interest, immediately shows the range of efficiencies wherein the support can be used when operated in columns of different lengths. When different columns are evaluated, the obtained kinetic plots show the range of plate numbers or analysis times wherein one column yields faster separations or produces more plates than another column. To obtain the ultimate performance limits of the column under consideration, the plots should be constructed for the largest possible ΔP-value (either the maximum pressure that the instrument can deliver or the maximum allowable pressure of the column). In this study, all columns were evaluated on traditional HPLC instruments, therefore the maximum available instrument pressure in the relevant formulas ($\Delta P = \Delta P_{max}$) was considered to be 400 bar.

For more explanation about the construction and interpretation of kinetic plots, the reader is kindly referred to some articles explaining the basics of the Kinetic Plot Method [14,15,18].

Kinetic plots of analysis time and column length *versus* the resolution of the critical pair have also been constructed. To the best of our knowledge this is the first time the resolving power of HPLC columns is evaluated by means of kinetic plots.

Typically, in pharmaceutical company practices, column selection is a step included in the method development strategy and it is most often aimed at differentiating bonded phase selectivities [19,20]. In this paper, instead, namely identical bonded phases (C18) have been considered and attention has been focused rather on the silica substrates of the packed columns that differ both in source material and geometrical features, being aware of the fact that the latter – affecting stationary phase bonding density, packing quality, mechanical and chemical resistivity and pressure drop – have a major contribution to the separation performance in terms of efficiency, analysis speed and bed permeability. Some differences in actual selectivity have nevertheless been observed between the different supports, resulting in a clear effect on their resolving power adding up to the effect of efficiency.

A particle analysis study was carried out in order to accurately determine the average particle sizes and relate them to the observed kinetic performances. Scanning electron microscopy (SEM) images for this particle analysis study were obtained in the backscattered electron mode in order to get a marked contrast that allowed to easily reprocess the images by image analysis software. The results obtained from the SEM images were subsequently compared with results obtained by laser light scattering (LLS) analyses.
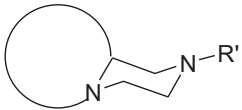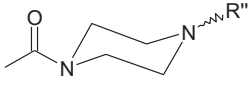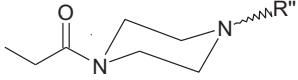
2. Experimental

2.1. Chemicals and columns

Uracil (≥99%), acetonitrile (gradient grade), ethanol (analytical grade) and acetic acid (glacial, 99.8%) were purchased from Sigma-Aldrich (Steinheim, Germany). Ammonium acetate (ACS, reagent) was purchased from Merck (Darmstadt, Germany). Deionized water (≤0.055 μS) was produced by MilliQ equipment (Millipore, Molsheim, France). The pharmaceutical compounds studied were provided by GlaxoSmithKline (Verona, Italy) and their main characteristics are summarized in Table 1.

The Hypersil Gold C18 column (150 mm × 4.6 mm, 3.0 μm) was purchased from ThermoFisher Scientific (Cheshire, UK), the ACE3 C18 column (150 mm × 4.6 mm, 3.0 μm) was purchased from Advanced Chromatography Technology (Aberdeen, UK), the XBridge C18 column (150 mm × 4.6 mm, 3.5 μm) from Waters (Milford, MA, USA) and the Gemini NX C18 column (150 mm × 4.6 mm, 3.0 μm) from Phenomenex (Torrance, CA, USA). Additional charac-

Table 1
Main physico-chemical characteristic of the pharmaceutical compounds used as test molecules.

Compound	Structure	Molecular weight (Da)	pK_a[a]	Log D[b]	Mobile phase pH[c]	D_M ($\times 10^{-10}$ m^2/s)
G1		669	2.0; 5.0	5.7	4.5	5.58
G2		616	7.1	5.4	8.0	5.84
G3		630	7.1	5.9	8.0	5.67

[a] pK_a-values measured from solubility data in saturated conditions and fitted by Kaleida Graph software.
[b] Lipophilicity, defined as Log of the distribution coefficient between aqueous phase buffered at pH 7.4 and n-octanol.
[c] Measured pH of the buffered aqueous component of the mobile phase.

teristics of the columns, from the manufacturer's claims, are shown in Table 2.

2.2. Apparatus and methodology

All experiments were conducted in the isocratic mode. Acetonitrile and 10 mM ammonium acetate (pH 4.5 for G1 and pH 8.0 for G2 and G3, respectively) were mixed by the HPLC pump in the ratio able to provide about the same retention factor for G1 ($k \cong 4.7$) in acidic conditions and G3 ($k \cong 3.9$) in basic conditions (see Table 3 for details). Van Deemter curves were constructed for every column at a temperature of 40 °C and for flow rates between 0.3 mL/min and the maximum flow rate obtained at 400 bar (depending on the permeability of the column, the maximum flow rate ranged between 3.7 mL/min and 4.7 mL/min). The viscosities of the used mobile phases were calculated according to Li and Carr [22]. The permeability of the columns was determined using Darcy's law, by measuring the pressure drop over the column at the highest linear velocity. Peak variances were calculated using the peak width at half height.

The experiments were performed on an Agilent 1100 HPLC system (Agilent Technologies, Waldbronn, Germany) equipped with a variable wavelength UV detector (14.0 μL flow cell, 10 mm path length), a thermostatted column compartment, a degasser and a quaternary pump. All connection tubing (diameter 120 μm) was

kept as short as possible to reduce extra-column band broadening. The total volume of the systems was determined to be 37 μL. The system was operated with Empower software. The maximum pressure on this system is 400 bar.

For the experiments under acidic conditions, samples consisting of 500 μg/mL uracil and 400 μg/mL G1 were dissolved in 50/50 (v%/v%) water/acetonitrile. The injected sample mixture volume was 2 μL. Absorbance values were measured at 260 nm with a sample rate of 40 Hz. For the experiments under basic conditions, samples consisting of 1000 μg/mL uracil and 1000 μg/mL G2 and G3 respectively were dissolved in 50/50 (v%/v%) water/acetonitrile. The injected sample mixture volume was 2 μL. Absorbance values were measured at 210 nm with a sample rate of 40 Hz.

All reported plate height and column permeability data were obtained after correction for the system band broadening (σ_{sys}^2), elution time (t_{sys}) and pressure drop (ΔP_{sys}), measured by removing the column from the system and replacing it with a zero-dead volume connection piece [23]. The subscript "total" refers to the experimentally measured efficiency, analysis time and pressure; the subscript "col" refers to the pure column efficiency obtained after correction:

$$N_{col} = \frac{(t_{R,total} - t_{R,sys})^2}{\sigma_{total}^2 - \sigma_{sys}^2} \tag{4}$$

Table 2
Characteristics of the columns under evaluation, from the manufacturers' claims.

Column	Dimensions (mm × mm)	Packing material	Particle diameter (μm)	Batch number	Pore size (Å)	Surface area (m^2/g)	Carbon load (%)
Hypersil Gold	150 × 4.6	High purity deactivated silica	3.0	9925	175	220	10
ACE3	150 × 4.6	High purity deactivated silica	3.0	V09-2156	90	400	20
XBridge	150 × 4.6	Hybrid	3.5	0107	135	185	18
Gemini NX	150 × 4.6	Hybrid	3.0	5560-32	110	375	14

Table 3
Chromatographic conditions and experimental data relevant to the evaluated columns. Viscosity and permeability values are averaged on experimental data from acidic and basic conditions.

Column	Mobile phase (acetate buffer/acetonitrile)	Mobile phase viscosity (mPa s)[a]	Retention factor (k_{G1})	Retention factor (k_{G2}, k_{G3})	Selectivity (α_{G3-G2})	Permeability ($\times 10^{-14}$ m^2)[b]
Hypersil Gold	41/59	0.54	4.7	3.7, 4.0	1.08	1.81
ACE3	35/65	0.50	4.7	3.6, 3.9	1.08	1.46
XBridge	37/63	0.52	4.6	3.4, 3.8	1.12	1.69
Gemini NX	34/66	0.50	4.4	3.4, 3.9	1.15	2.07

[a] Values calculated from [21].
[b] Values calculated from experimental data at maximum operated pressure and 40 °C.

$$H_{col} = \frac{L}{N_{col}} \tag{5}$$

$$K_{v0} = \frac{u_0 \eta L}{(\Delta P_{total} - \Delta P_{sys})} \tag{6}$$

2.3. Solid state measurements

To determine the true particle size of the studied columns, the columns were opened after the separation experiments and the particles were removed by gently flushing the columns with ethanol. The particles were subsequently dried by evaporating the ethanol at room temperature in the fume hood and prepared for SEM and LLS measurements. The SEM pictures were recorded with a Quanta FEG 200 instrument equipped with a Field Emission Gun source. The microscope was operated at 20 kV with a magnification of 3500× and a backscattered electrons detector (BSED) to obtain enhanced contrast conditions. The particles were conductive enough to omit the use of a conductive coating layer and they were analyzed onto a self-adhesive carbon sample holder. At least four pictures for three aliquots of each sample were taken and 800 particle diameters were measured for every column by re-processing the images with the CLEMEX PS^3 image analysis software in order to determine the true diameter and roundness of the analyzed particles. The LLS measurements were performed with a Sympatec Helos KF instrument in dry mode by using the Aspiros as dispersion unit. The measurement settings were: 1 bar pressure and a measurement range between 0.45 and 87.5 μm. The reported results are the X50 value for the LLS technique and the D50 value for the image analysis.

3. Results and discussion

Experimental van Deemter curves and kinetic plots, constructed at pH 4.5 and pH 8.0 in analogous chromatographic conditions are commented in the next paragraphs. Efficiency and analysis speed were first derived and related to the results from the particle analysis at pH 4.5. Theoretically, efficiency and column bed permeability changes are not expected when changing pH, if considering ideally inert stationary phases and neutral analytes interacting only through hydrophobic forces. Nevertheless, in practice, discrepancies from theory are particularly likely to rise at basic pH, where possible unshielded silanol groups are deprotonated and can give rise to secondary interactions with the analytes.

3.1. Comparison of column performance at pH 4.5

3.1.1. Van Deemter plots

Fig. 1 shows the experimentally obtained van Deemter curves for G1 in acidic elution conditions on the different evaluated support types. In the mobile phase conditions used for all columns (Table 3) the molecule is neutral. This is demonstrated by UV spectra (data not shown) and chromatographic data and is despite the fact that the pH of the aqueous buffer (pH 4.5) before mixing with the organic modifier (acetonitrile) is lower than the molecule's pKa-value (pKa = 5.0). This is due to both the change of the degree of ionization of the molecule in the hydro-organic environment, with respect to its ionization in pure water, and to the change of apparent pH observed in anionic buffers upon the addition of acetonitrile. It is in fact proven that, on one hand, bases show lower pKa-values in a hydro-organic environment, independently of the solvent used [24], and, on the other hand, an increase of up to 2 units in apparent pH is achieved for anionic buffers upon the addition of about 60% acetonitrile [25]. The experimental conditions chosen thus ensure the neutrality of the molecule in the mobile phase and, as a consequence, the absence of undesired ionic interactions with the stationary phase.
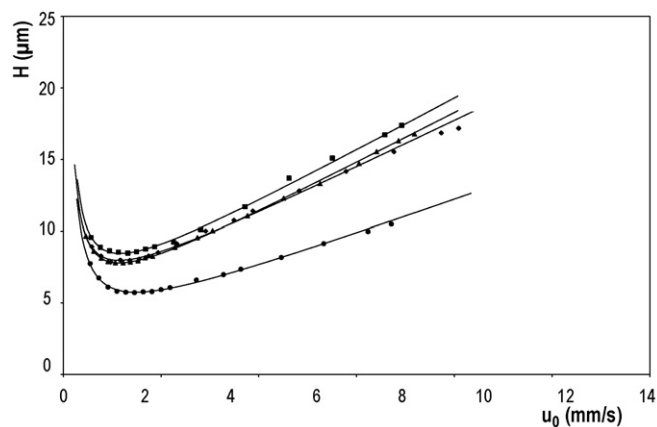

Fig. 1. Experimentally obtained van Deemter curves for G1 at pH 4.5 on (▲) Hypersil Gold C18 (d_p = 3.0 μm), (●) ACE3 C18 (d_p = 3.0 μm), (■) XBridge C18 (d_p = 3.5 μm) and (♦) Gemini NX C18 (d_p = 3.0 μm). For each of these columns, the mobile phase composition was adjusted to obtain the same retention factor for G1 (k = 4.7 ± 0.2) (see Table 3).

The diffusion coefficient of the molecule in the mobile phases used was determined to be 5.58×10^{-10} m^2/s, using the Wilke-Chang correlation [21]. The slight changes in mobile phase composition, made to obtain the same retention factor on the different columns, hence did not affect the diffusion coefficient significantly.

Fig. 1 shows that a clear distinction in performance can be made between the Hypersil Gold, XBridge and Gemini NX columns on one hand, and the ACE3 column on the other hand. Whereas Hypersil (d_p = 3.0 μm) and Gemini NX (d_p = 3.0 μm) have a minimum plate height of 7.7 μm and XBridge (d_p = 3.5 μm) has a minimum plate height of 8.5 μm (corresponding to a minimum reduced plate height (h_{min}) of 2.5 for all), the ACE3 column clearly performs better with a minimum plate height of 5.8 μm (corresponding to a h_{min} of 1.9). Well performing columns in general have a minimum reduced plate height of 2. The ACE3 column can therefore be said to have an excellent efficiency. The reduced minimum plate heights were calculated using the particle diameter provided by the manufacturers.

Comparing the permeability (K_{v0}) values of the 3.0 μm supports (see Table 3), it can furthermore be noted that the ACE3 column has a lower permeability than the Gemini NX and Hypersil Gold columns. This can indicate a smaller average particle size of the packing.

3.1.2. Efficiency and analysis speed

A useful tool to compare column performance under different chromatographic conditions or evaluated with different compounds is the kinetic plot of t_0 versus N, where t_0 is the elution time of an unretained peak (uracil) and N is the plate count of the tested molecule. This kind of plot allows the chromatographer to gather information on the intrinsic kinetic performance of one or more columns, independent of their selectivity and the chromatographic conditions. In Fig. 2, kinetic plots of time (t_0) versus efficiency (N) are shown for the data obtained in Fig. 1. The corresponding retention time of a compound of interest can be calculated from these plots using the retention factor k of this compound (Table 3):

$$t_R = t_0(1 + k) \tag{7}$$

From the plots, the range of efficiencies wherein a certain support performs better than another can be determined at a glance. The plots in Fig. 2 were obtained for a maximum pressure of 400 bar, as this is the maximum pressure the columns can be operated at.

The ACE3 column clearly performs better than the other supports for the entire range of practically relevant plate counts
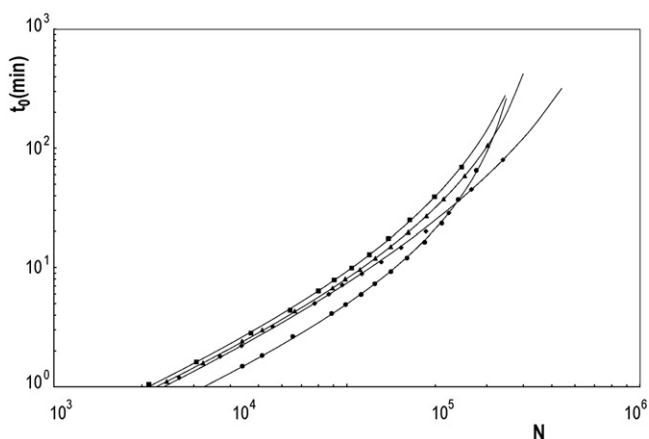
Fig. 2. Kinetic plots of analysis time (t_0) versus efficiency (N) obtained for the supports evaluated in Fig. 1. Same symbols are used as in Fig. 1.

Table 4
Particle size values obtained with SEM Image and LLS analysis, total porosity values (ε_T), reduced minimum plate heights (h_{min}) and flow resistances (ϕ_0).

Particle size distribution							
Column	Average diameter (μm) (SEM)	Roundness	D50	X50	ε_T	h_{min}	ϕ_0
Hypersil Gold	4.0	0.90	4.0	4.3	0.66	2.0	878
ACE3	3.5	0.92	3.4	3.6	0.55	1.6	828
XBridge C18	3.9	0.92	3.8	4.0	0.54	2.2	881
Gemini NX	3.4	0.90	3.4	3.3	0.52	2.3	588

(10,000 < N < 250,000), achieving separations faster at any given efficiency in the specified range. Whereas the better efficiency of the ACE3 columns was already assessed from Fig. 1, Fig. 2 now directly shows what gain in t_0-time, and hence analysis time via Eq. (7), can be obtained by using an ACE3 support instead of, e.g. a Gemini NX support. An efficiency of N = 50,000 plates, can for example be obtained with the ACE3 column in only 10 min for G1 (k = 4.7, cf. Eq. (7)), while it takes 15 min to obtain the same efficiency on the Gemini NX column (k = 4.4, cf. Eq. (7)).

For very high efficiencies (plate counts higher than 250.000), the Gemini NX outperforms all tested fully porous columns, showing lower t_0-times. This is directly related to its high permeability (1.97×10^{-14} m²/s, see Table 3) that allows overcoming the pressure drop limitation that usually impairs the achievement of the highest efficiencies, for which very long columns are needed.

3.1.3. Reduced kinetic plots

To assess the quality of a packing without having to specify a mean particle diameter or reference length, the use of reduced kinetic plots has been proposed in Refs. [14,26]. These reduced kinetic plots are obtained by plotting the separation impedance (E_0) versus the plate number ratio (N/N_{opt}) for the support under consideration:

$$E_0 = \frac{H^2}{K_{v0}} = h^2 \phi \tag{8}$$

$$\frac{N}{N_{opt}} = \frac{u_{opt} H_{min}}{u H} = \frac{v_{opt} h_{min}}{v h} \tag{9}$$

Both quantities are only dependent on the dimensionless variables h (the reduced plate height, $h = H/d_p$), v (the reduced mobile phase velocity, $v = u_0 \times H/D_m$, with D_m the molecular diffusion coefficient (m²/s) and ϕ (the flow resistance, $\phi = dp^2/K_{v0}$) and can be calculated, as can be inferred from Eqs. (8) and (9), without having to specify the actual size of the particles. This obviously excludes a number of important error sources. A reduced kinetic plot hence yields the same type of information as a reduced van Deemter plot: packings with the same packing quality, intra-particle diffusion characteristics and the same retention factor but a different size will yield coinciding curves. The lower this curve, the better packed the column will be. The reduced kinetic plot, however, has a second important advantage over the reduced van Deemter plot in that it also incorporates information on the flow resistance. In fact, the plot shows how E_0 varies with N and E_0 has traditionally been used as a measure for packing quality [27,28]. To compare the packing quality of the supports discussed in Fig. 1, plots of E_0 versus N/N_{opt} were constructed using Eqs. (8) and (9) and are shown in Fig. 3a.

Fig. 3a shows that ACE3 clearly is the best packed column in this ranking, having $E_{0,min}$ = 2200. The other columns follow the same trend as in Fig. 2, therefore the performance of the columns is clearly related to their packing quality. The separation impedance values used to construct the plots in Fig. 3a are calculated using the permeability values obtained from the linear velocity (Eq. (6)). Using the separation impedance based on the permeability obtained from the interstitial velocity instead of the linear velocity allows accounting for differences in porosity between the supports. The so-called interstitial permeability based separation impedance (E_i) can be calculated from the experimentally determined value of K_{v0} and the total (ε_T) and external porosity (ε_e) as follows:

$$E_i = \frac{H^2}{K_{Vi}} = \frac{H^2}{K_{v0}} \frac{\varepsilon_e}{\varepsilon_T} \tag{10}$$

The total porosity of the columns was determined from the elution time of uracil, after correction for the extra-column contribution. The values of ε_T are shown in Table 4. All investigated columns have a total porosity that is close to 0.55. The only column with a significantly different value is the Hypersil Gold column. For the external porosity, a general value of ε_e = 0.38 was assumed for all columns. Changing this value between ε_e = 0.36 and ε_e = 0.42 (the generally assumed minimum and maximum external porosity values that can be expected for a packed bed column) did not affect the order of the curves.

With these values of ε_T and ε_e the impedance plots based on the interstitial permeabilities shown in Fig. 3b were constructed. Although the general order of the packings remains the same in both figures, the comparison of Fig. 3a and b shows that the large total porosity (ε_T) of the Hypersil Column somewhat impairs its performance (the performance of the column clearly improves when the large ε_T is filtered out in Fig. 3b). Assuming that all columns have a similar external porosity, the large total porosity of the Hypersil column must be due to a large internal porosity (ε_i):

$$\varepsilon_i = \frac{\varepsilon_T - \varepsilon_e}{1 - \varepsilon_e} \tag{11}$$

an assumption that is confirmed by the large pore size of the packing material (175 Å versus 90 Å–135 Å for the other supports). The comparison of Fig. 3a and b hence shows that the observed differences in performance of the packing materials can partly be explained by differences in porosity.

To relate the observed ranking in performance of the different supports to the true particle size of the packings, a particle analysis study was conducted by means of SEM and LLS, as described in Section 2.

3.1.4. Particle analysis

The particle size distribution (PSD) and average particle diameter of the packing materials were measured from SEM pictures elaborated by CLEMEX PS³ image analysis software. At least 800 particles were analyzed for each column. In addition, the particle roundness was calculated from image analysis. The PSD results from the image analysis were compared with the PSD results from
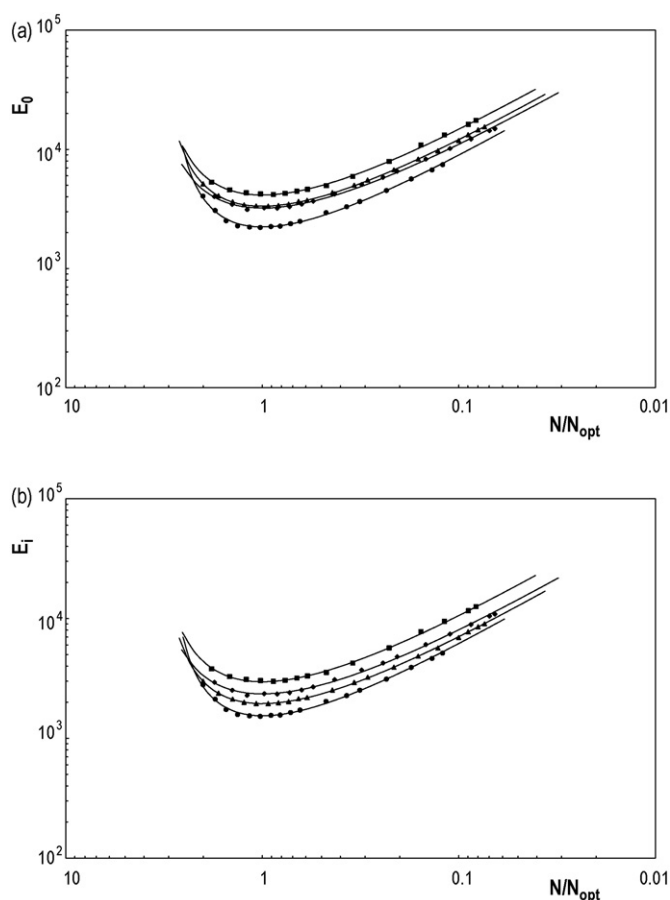
Fig. 3. Reduced kinetic plots of (a) E_0 *versus* N/N_{opt} and (b) E_i *versus* N/N_{opt} obtained for the supports evaluated in Fig. 1 by using Eqs. (8)–(10). For each of these columns, the mobile phase composition was adjusted to obtain the same retention factor for G1 ($k = 4.7 \pm 0.2$) (see Table 3). Same symbols are used as in Fig. 1.

the LLS analysis. Table 4 lists the average particle diameter, the roundness of the particles and the D50-values obtained from the SEM analysis and the X50-values obtained by the LLS experiments. Both D50 and X50 indicate the 50th percentile, i.e. the particle size below which it is possible to find 50% of the particle distribution, obtained by SEM pictures image analysis and LLS, respectively. Because the LLS technique approximates the scattering intensities of the particle to that of a sphere of equal volume, a discrepancy might be observed between the D50 and X50-values if the particles are not perfectly round. In addition, it is assumed in the current experimental set-up that no light absorption occurs from the scattering material, based on the Fraunhöfer theory. This assumption can lead to an additional discrepancy between the D50-values of the Image analysis and the X50-values of the LLS analysis. The good agreement found between the two independently obtained distribution parameters for the studied particles (Table 4), however, supports the validity of the LLS assumptions and the reliability of the results. The roundness values additionally confirm that all suppliers provide almost perfectly spherical particles.

The average particle diameters were subsequently determined from the SEM analysis and amounted $4.0\,\mu m$ for Hypersil Gold, $3.5\,\mu m$ for ACE3, $3.9\,\mu m$ for the XBridge support and $3.4\,\mu m$ for Gemini NX (Table 4). These values are in excellent agreement with the D50- and X50-values determined previously, but are clearly larger than the values specified by the manufacturers. This might be due to the fact that different techniques (e.g. Coulter counting, which is known to underestimate the size of porous particles [29]) were used to determine the average particle diameter. From these values, it is also evident that ACE3 does not have the smallest particle size, as was assumed from the lower H_{min} and permeability

values in Section 3.1.1, but that its better performance is due to its better packing quality, as shown in Fig. 3.

With the true particle size, the actual minimum plate heights and flow resistances can now be calculated. These values are also shown in Table 4. The obtained values explain the observed ranking of the curves in Fig. 3: The excellent efficiency of the ACE3 column ($h_{min} = 1.6$) and average flow resistance make it the best performing column in the impedance plot. The relatively poor efficiency of the Gemini NX column is compensated by its very low flow resistance, making it the second best performing column in Fig. 3. The fact that the XBridge column has the lowest h_{min} value and the highest flow resistance, make it least well performing column of the evaluated supports. This ranking is again also directly visible in Fig. 2.

### 3.2. Comparison of column performance at pH 8.0

3.2.1. Van Deemter plots

For the aim of the present work, the columns under evaluation were also tested under basic conditions, namely in pH 8.0 acetate buffer, using a probe molecule (G3) with a very similar diffusion coefficient D_M, molecular weight (MW) and hydrophobicity (Log D) as G1. G3 has a pK_a equal to 7.0, ensuring neutrality in the mobile phase employed.

Fig. 4 shows the van Deemter curves that were obtained for G3 on the different supports and Table 5 shows the minimum plate heights obtained at both pH's for all columns. Compared with the evaluation at pH 4.5, the efficiency of the ACE3, XBridge and Gemini NX columns remains mainly unchanged (the plate heights at both pH values are within 10% of each other). The Hypersil Gold column, however, displays a strong decrease in efficiency at pH 8.0
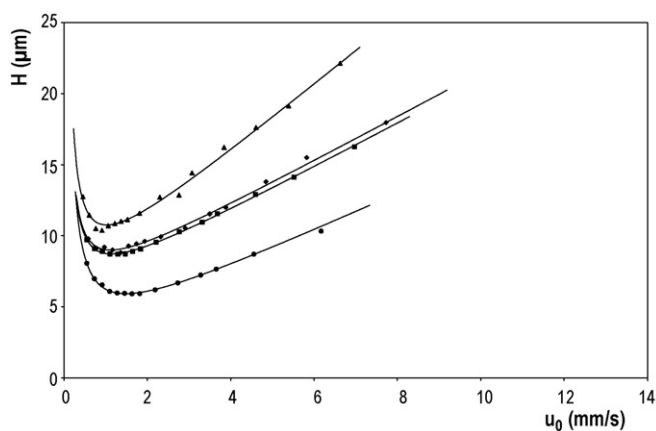
Fig. 4. Experimentally obtained van Deemter curves for G3 at pH 8.0. For each of these columns, the mobile phase composition was adjusted to obtain the same retention factor for G3 ($k = 3.9 \pm 0.1$) (see Table 3). Same symbols are used as in Fig. 1.
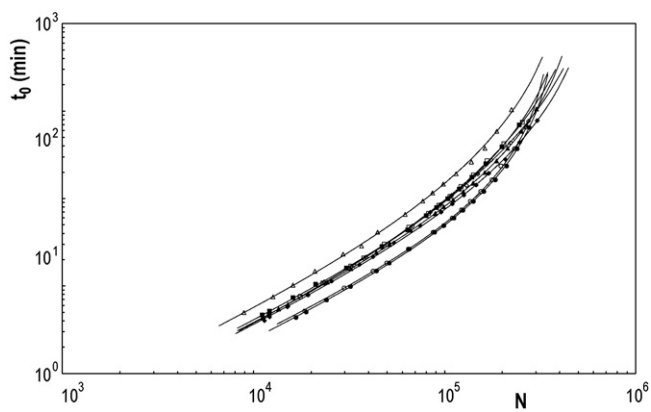
Fig. 5. Kinetic plots of analysis time (t_0) *versus* efficiency (N) obtained from the van Deemter data of the evaluated supports at pH 4.5 and 8.0 (see Figs. 1 and 4). Same symbols are used as in Fig. 1, the full symbols correspond with the data obtained at pH 4.5, while the open symbols correspond with the data obtained at pH 8.0.

compared to pH 4.5. After the analysis at pH 8.0, the Hypersil Gold column was retested at pH 4.5 using G1 as test compound and the obtained efficiencies were still comparable to what was observed during the first experiments at pH 4.5. This indicates that the bad performance observed at pH 8.0 was not due to an overall column failure, but rather to a clear efficiency loss at high pH, in spite of the manufacturer's claim of suitability up to pH 12. This observation can be explained by the presence of un-protected silanols on the silica surface, due to incomplete or poorly efficient de-activation and end-capping processes.

3.2.2. Efficiency and analysis speed at basic pH

As already mentioned in Section 3.1.2, the best tool to compare column performance under different chromatographic conditions or evaluated with different compounds is the kinetic plot of t_0 *versus* N. As the columns were evaluated with different compounds (G1

Table 5
Obtained minimum plate heights (H_{min}, μm) for the column evaluation made with G1 at pH 4.5 and G3 at pH 8.0.

| Column name	pH 4.5	pH 8.0
Hypersil Gold C18	7.8	10.4
ACE3 C18	5.7	5.9
XBridge C18	8.5	8.7
Gemini NX C18	7.9	8.8

at pH 4.5 and G3 at pH 8.0), plots of t_0 *versus* N were constructed in Fig. 5 to compare the kinetic performance of the columns at the two pH's. From these plots, it can be assessed that the ACE3, XBridge and the Gemini NX curves perfectly overlap, whereas the Hypersil Gold column actually shows some discrepancies in performance at pH 4.5 and 8.0. The loss in efficiency for this column was already apparent from the van Deemter plots in Fig. 4 and it is now also reflected in the kinetic plot.

It can thus be concluded that hybrid silica supports preserve their efficiency in the entire suitable pH range and are not particularly affected by the usually detrimental secondary interactions that may appear at high pH. For the ultra-high purity silica columns, however, it seems that the performance of the columns at high pH mainly depends on the manufacturer's ability and technical result of the de-activation and end-capping processes.

3.2.3. Resolution comparison

From the kinetic performance plots assessed so far, further information that can be valuable to a chromatographer can easily be derived. For example, information on the resolution between two different compounds investigated under the same separation conditions can be obtained and the minimum column length or minimum analysis time to obtain their baseline separation can be forecast.

This type of experiment was conducted in order to investigate the resolution between G3 and its related impurity G2 at pH 8.0. The (u_0, H)-plots of both molecules can easily be transformed in plots of analysis time *versus* resolution or column length *versus* resolution,
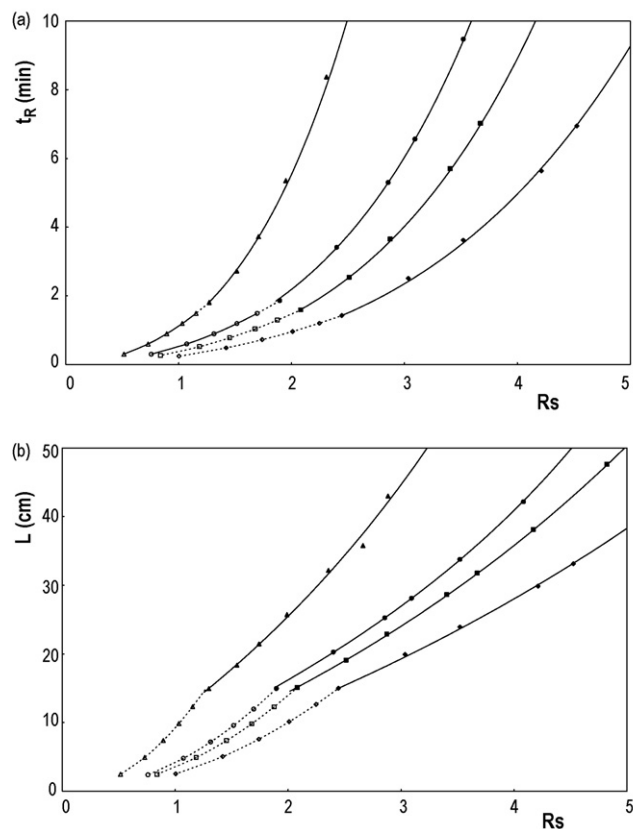
Fig. 6. Kinetic plots of (a) analysis time *versus* resolution (R_s) and (b) column length (L) *versus* resolution (R_s) obtained for the critical pair consisting of G2 and G3. The mobile phase was chosen in such a way that the k for G3 was the same on all evaluated supports ($k = 3.9 \pm 0.1$) (see Table 3). Same symbols are used as in Fig. 1. The dashed lines and open symbols correspond with the resolution that is obtained when an upper limit is set on the linear velocity ($u_0 \leq u_{0,max}$, with $u_{0,max}$ the maximum experimentally determined velocity).
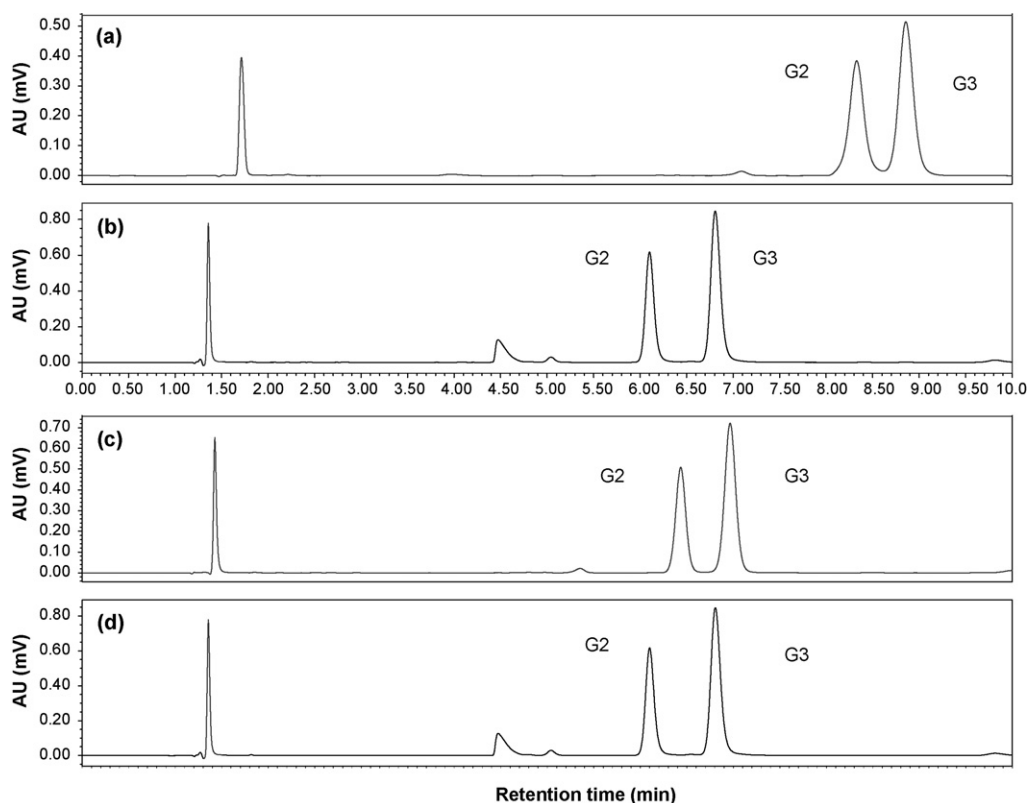
Fig. 7. Chromatograms of G2 and G3 on (c) Hypersil Gold C18, (d) ACE3 C18, (a) XBridge C18 and (b) Gemini NX C18 in isocratic conditions; mobile phase 10 mM acetate buffer pH 8.0/acetonitrile (percentage composition as in Table 3), flow 1 mL/min, detection wavelength 210 nm. The first eluting peak in all chromatograms is uracil (unretained molecule).

provided the retention factors, k, of both molecules are known. Resolution plots were constructed for each column under evaluation by calculating the resolution of the two compounds at every flow rate using the following expression:

$$R_s = \frac{1}{2} \frac{(k_2 - k_1)}{(1 + k_1/\sqrt{N_1}) + (1 + k_2/\sqrt{N_2})} \qquad (12)$$

In the resulting resolution plots shown in Fig. 6, the differences in selectivity of the various columns are combined with the differences in efficiency. As the mobile phase compositions were already selected such as to keep the retention factor for G3 the same on every column type, the retention factors obtained for G2 on the different columns, immediately indicate any possible difference in selectivity for G2 between the different supports. The retention factors obtained for compounds G2 and G3 and their selectivity factors α are shown in Table 3. For XBridge and Gemini NX, the observed selectivity factors are larger than 1.1. The Hypersil Gold column and ACE3 column, however, have a significantly lower selectivity for this specific critical pair ($\alpha = 1.08$). It must be noted here that the resolution changes observed along the kinetic plot curve of every column are associated exclusively with the changes in efficiency obtained upon changing the flow rate. This is because the retention factors, and hence the selectivity, in principle do not change when changing the flow rate or the length of the support. The resolution differences between the various columns, on the other hand, are associated with their intrinsic differences in selectivity and efficiency. Sample chromatograms obtained for the four columns at the same flow rate (1 mL/min) are presented in Fig. 7.

The lowest resolution factors shown in Fig. 6a and b were obtained in columns that are exactly long enough to yield the maximum experimentally determined linear velocity ($u_{0,max}$) at the maximum pressure. For the supports considered here, these minimum resolution factors are well above $R_s = 1.5$, except for the Hypersil column (minimum $R_s = 1.3$). To get an idea of what column lengths or analysis times are needed to obtain a resolution factor of 1.5, an extrapolation can be made to shorter column lengths. Inherent to the KPM, however, the performances of these shorter column lengths should be calculated for velocities that are higher than $u_{0,max}$. These points are based on the extrapolation of the plate height fittings in the C-term dominated range of Fig. 4 and can therefore be subjective to the extrapolation error that goes with all existing van Deemter curve-fitting models. To avoid such errors, a constraint was imposed to the linear velocity to ensure that none of the considered supports was allowed to work at a velocity larger than that for which an experimental measurement is available [30]. Practically, this means that columns that are shorter than the column length that results in $u_{0,max}$ at the maximum pressure, will be operated at the same velocity but at pressures that are lower than the maximum pressure. Provided that the plate height of the column does not change with the column length, this approach will lead to safe extrapolations. The lengths of the resulting columns can be calculated as:

$$L_{var} = \frac{\Delta P_{var}}{\eta} \frac{K_{v0}}{u_{0,max}} \qquad (13)$$

for values of the pressure (ΔP_{var}) that are varied in a linear and equidistant way between the maximum pressure and 0.

The plate counts of these columns were then determined as $N = L_{var}/H_{max}$ where H_{max} is the plate height corresponding with $u_{0,max}$. Finally the corresponding analysis times were calculated as $t_0 = L_{var}/u_{0,max}$. For these shorter columns, the expected resolutions were again calculated using Eq. (12) and are shown in Fig. 6a and b (dashed lines and open symbols).

Assuming now that a minimum resolution of 1.5 is required for the baseline separation of G2 and its related impurity G3, the analy-

sis time that will result in this baseline separation can immediately be read out from Fig. 6a. The Gemini will achieve a baseline separation in 0.6 min, due to its excellent selectivity for the critical pair combined with its high permeability. To gain the same resolution, 0.9 min, 1.3 min and even 2.7 min are needed on XBridge, ACE3 and Hypersil. The column lengths corresponding with these resolutions can be directly read out from Fig. 6b.

The KPM approach appears hence to be a valuable tool to forecast column performance and the minimum required column length or analysis time for difficult separations, optimizing kinetic conditions of separation. It should, however, be kept in mind that the results obtained in this study are related to pharmaceutical nitrogen-containing weak bases of given size and diffusion coefficient. Therefore, the observed behaviour of the different columns might be different when evaluating different compounds. Also, the scope of this study was to show how different supports can be evaluated for a specific separation case using the KPM, and for this purpose only one column of every manufacturer was compared. It is of course possible that different results will be obtained if a larger number of different batches would be evaluated for every manufacturer.

4. Conclusions

Four types of fully porous C18 columns of different manufacturers were compared by means of the KPM, two based on ultra-pure silica supports and two based on hybrid polymeric silica materials. For the column comparison, nitrogen-containing pharmaceutical compounds of medium size (ca. 600 Da) and medium lipophilicity (Log D between 5 and 6) were considered. The column evaluation was performed both at pH 4.5 and 8.0. Kinetic plots of efficiency *versus* analysis time were used to directly determine which support would yield a certain efficiency in the shortest possible analysis time in both conditions sets.

Considerations drawn at pH 4.5 were directly related to the support's geometrical characteristics, as the stationary phases are ideally inert in these conditions and supposed to interact with neutral analytes only through hydrophobic forces. Under these circumstances a clear ranking in performance could be observed for the different support types, with ACE3 displaying the best performance, XBridge the least good and Hypersil Gold and Gemini NX an intermediate performance, despite roughly identical nominal particle diameter. This ranking in performance could be directly related to the flow resistance and minimum plate heights of the different supports, determined from the true particle size obtained from SEM pictures using image analysis.

The efficiency evaluation of the different supports at basic pH (pH 8.0) showed the same efficiency for polymer-silica supports but a significant loss of performance for the Hypersil Gold column, and this might be related to a less efficient de-activation process of the silica that leaves unshielded silanol groups on the surface.

The resolution between two pharmaceutical compounds at pH 8.0 was determined by means of kinetic plots of resolution *versus* length and resolution *versus* analysis time. Due to significant differences in intrinsic selectivity between the supports, it could be determined that Gemini NX would lead to the fastest baseline separation of the critical pair, followed by XBridge, ACE3 and Hypersil Gold, in spite of nominally identical bonded phases (C18). The resolution kinetic plots are moreover well suited to assess what column length should be used to obtain a baseline separation for

a critical pair and in what analysis time full separation will be obtained.

A remark that must be made is that the resolution plots (and all other kinetic plots in the manuscript) have been constructed for data that have been corrected for extra-column band broadening and hence reflect the pure column performance. However, when supports are pushed to their highest level of kinetic performance, hence in very short columns at high velocities, the effect of extra-column band broadening will become more important and cannot always be ignored. Kinetic plots that incorporate these extra-column effects can be constructed by incorporating the expression for the extra-column contribution in the kinetic plot equations. This has been demonstrated by Fountain et al. [31].

References

[1] J.W. Li, P.W. Carr, Anal. Chem. 69 (1997) 2193.
[2] T.P. Weber, P.T. Jackson, P.W. Carr, Anal. Chem. 67 (1995) 3042.
[3] C. Zhu, D.M. Goodall, S. Wren, LC–GC Eur. 10 (2004) 530.
[4] F. Gritti, G. Guiochon, Anal. Chem. 77 (2005) 1020.
[5] D.V. McCalley, Anal. Chem. 75 (2003) 3404.
[6] N.H. Davies, M.R. Euerby, D.V. McCalley, J. Chromatogr. A 1178 (2008) 71.
[7] N. Lindegard, T.T. Hien, J. Farrar, P. Singhasivanon, N.J. White, N.P.J. Day, J. Pharm. Biomed. Anal. 42 (2006) 430.
[8] R.C. Duca, F. Bravin, M. Delaforge, L. Vladescu, I.A. Badea, R.D. Criste, J. Agric. Food Chem. 57 (2009) 10497.
[9] S.j. Mayatra, B. Prasad, M. Jain, R. Jain, S. Singh, J. Pharm. Biomed. Anal. 52 (2010) 410.
[10] Q. Fu, M. Shou, D. Chien, R. Markovich, A.M. Rustum, J. Pharm. Biomed. Anal. 51 (2010) 617.
[11] J. Zheng, D. Patel, Q. Tang, R.J. Markovich, A.M. Rustum, J. Pharm. Biomed. Anal. 50 (2009) 815.
[12] M. Molikova, P. Jandera, J. Sep. Sci. 33 (2010) 453.
[13] C.E. Jones, C.J. Darcy, T. Woodberry, N.M. Anstey, Y.R. McNeil, J. Chromatogr. B 878 (2010) 8.
[14] G. Desmet, D. Clicq, P. Gzil, Anal. Chem. 77 (2005) 4058.
[15] G. Desmet, P. Gzil, D. Clicq, LC–GC Eur. 7 (2005) 403.
[16] D. Cabooter, A. de Villiers, D. Clicq, R. Szucs, P. Sandra, G. Desmet, J. Chromatogr. A 1147 (2007) 183.
[17] D. Cabooter, F. Lestremau, F. Lynen, P. Sandra, G. Desmet, J. Chromatogr. A 1212 (2008) 23.
[18] U.D. Neue, LC–GC Eur. 22 (2009) 570.
[19] R.M. Krisko, K. McLaughlin, M.J. Koenigbauer, C.E. Lunte, J. Chromatogr. A 1122 (2006) 186.
[20] K.P. Xiao, F.Z. Liu, A.M. Rustum, J. Chromatogr. A 1163 (2007) 145.
[21] C.R. Wilke, P. Chang, AICHE J. 1 (1955) 264.
[22] J. Li, P.W. Carr, Anal. Chem. 69 (1997) 2530.
[23] D. Guillarme, S. Heinisch, J.L. Rocca, J. Chromatogr. A 1052 (2004) 39.
[24] S. Pous-Torres, J.R. Torres-Lapasio, J.J. Baeza-Baeza, M.C. Garcıa-Alvarez-Coque, J. Chromatogr. A 1163 (2007) 49.
[25] X. Subirats, E. Bosch, M. Rosès, J. Chromatogr. A 1059 (2004) 33.
[26] J. Billen, D. Guillarme, S. Rudaz, J.-L. Veuthey, H. Ritchie, B. Grady, G. Desmet, J. Chromatogr. A 1161 (2007) 224.
[27] U.D. Neue, HPLC columns: Theory, Technology and Practice, Wiley-VCH, New York, 1997.
[28] P.A. Bristow, J.H. Knox, Chromatographia 10 (1977) 279.
[29] T. Allen, Particle Size Measurement, Chapman and Hall, London, 1968.
[30] G. Desmet, D. Clicq, D. Nguyen, D. Guillarme, S. Rudaz, J.L. Veuthey, N. Vervoort, G. Torok, D. Cabooter, P. Gzil, Anal. Chem. 78 (2006) 2150.
[31] K.J. Fountain, U.D. Neue, E.S. Grumbach, D.M. Diehl, J. Chromatogr. A 1216 (2009) 5979.